Ultrafast Triplet State Formation in a Methylated Fungi-Derived Pigment: Towards Rational Molecular Design for Sustainable Optoelectronics

Taylor D. Krueger,[a] Longteng Tang,[a] Gregory Giesbers,[b] Ray C. Van Court,[c] Liangdong Zhu,[a] Seri C. Robinson,[c] Oksana Ostroverkhova,[b] and Chong Fang*,[a]

[a] Department of Chemistry, Oregon State University, 153 Gilbert Hall, Corvallis, Oregon 97331, United States

[b] Department of Physics, Oregon State University, 301 Weniger Hall, Corvallis, Oregon 97331, United States

[c] Department of Wood Science and Engineering, Oregon State University, 119 Richardson Hall, Corvallis, Oregon 97333, United States

* To whom correspondence should be addressed. E-mail: Chong.Fang@oregonstate.edu

Abstract. Organic triplet-generating materials have prolonged excited-state lifetimes that could enhance photocatalysis, light-emitting diodes, and versatile optoelectronics. Dimethylxylindein, a methylated derivative of a naturally sourced electronic material, xylindein, generates detectable triplet states upon photoexcitation in solution. Femtosecond transient absorption measurements of dimethylxylindein demonstrate that bluer excitation wavelengths enhance the intersystem crossing (ISC) in dichloromethane (DCM) which reduces the photostability compared to robust xylindein. No appreciable triplet states are generated in the more polar ethanol or thin films. The methoxy groups open two ISC pathways: one ultrafast (~140 fs) and one slower (~20 ps), the latter process enhanced by nonplanar structural motions that promote spin-orbit coupling over the chromophore ring-conjugated framework. Tunable femtosecond stimulated Raman spectroscopy (FSRS) and systematic quantum calculations characterize a light-induced charge-transfer state that becomes more stabilized in polar solvents like ethanol to quench ISC. In thin films, though the stabilized charge-transfer state on ultrafast timescales may promote photosensitivity, the triplet yield could be boosted via rational design strategies including thionation and implementation of heterocyclic nitrogen to broaden the sustainable optoelectronic applications of xylindein derivatives.

KEYWORDS: *Chlorociboria* fungi-derived pigment, excited state dynamics, femtosecond laser spectroscopy, intersystem crossing, intramolecular charge transfer, optoelectronic material

1. INTRODUCTION

Organic chromophores for optoelectronic materials are highly sought after due to their versatility and appealing properties for applications from quantum and optical computing, nanophotonic devices, high-speed telecommunications, to photovoltaics.[1-5] Many organic pigments have large polarizabilities, low dielectric constants, and inherent flexibility with ultrafast response time (e.g., femtosecond, 10^{-15} s) leading to higher device bandwidths.[6,7] Triplet states in organic electronic materials also play a significant role, contributing to both device performance and stability.[8] For example, chromophores with accessible triplet states may increase the probability for charge separation and capture due to long excited-state lifetimes and carrier diffusion lengths.[9,10] In particular, triplet excitons can have diffusion lengths ranging from ~30–300 nm, much longer than singlet excitons with typical diffusion lengths of ~5–20 nm.[3,11,12] Some light-harvesting materials exploit these properties, though they often rely on heavy-metal complexes with more intense spin-orbit coupling (SOC) to enhance intersystem crossing (ISC). Achieving these properties with organic chromophores is desirable due to their availability and simple processing requirements that could be upscaled for mass production.[13] In addition to the reduced cost compared to inorganic counterparts, environmental concerns from the processing and waste of metals (e.g., toxicity) is alleviated when working with organic chromophores. Many of these pigments contain nitrogen heterocyclic aromatics and carbonyl groups because the orbital mixing provided by the non-bonding (n) orbitals improves SOC. According to the El-Sayed rule,[14] ISC is allowed when the transition involves a change in electronic configuration and orbital type (e.g., $n\pi^* \leftrightarrow \pi\pi^*$).[15,16] Generally speaking, the topic of what factors control triplet formation in organic chromophores that do not contain heavy atoms, and therefore do not engage in the common SOC interactions that make metal complexes appealing as sensitizers, is presently a compelling research topic of interest.

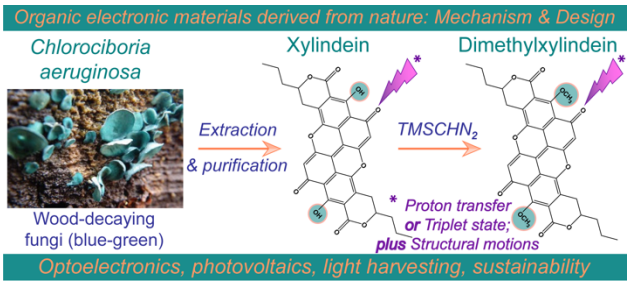

Scheme 1. Sample molecules derived from the wood-decaying fungi *Chlorociboria aeruginosa.* Following harvest, the cultures were lab-grown before xylindein was extracted and purified. The methylating agent trimethylsilyldiazomethane ($TMSCHN_2$) was reacted with xylindein to yield dimethylxylindein for ensuing spectroscopic investigations. The asterisks by the lightning symbol (depicting photoexcitation) highlight distinct processes of xylindein (excited-state intramolecular proton transfer) *vs.* dimethylxylindein (triplet formation) besides common structural motions.

A multidisciplinary approach enabled development of an efficient protocol from the growth, extraction, and purification to produce xylindein.[17-21] With a broad absorption profile, xylindein shows promise as an organic π-conjugated material with competitive electron mobilities and conductivity. Excimer formation in xylindein thin films quenches the excited state, benefiting (photo)stability but limiting charge transfer (CT); the stability in solution is maintained by an ultrafast excited-state intramolecular proton transfer (ESIPT) and nonradiative relaxation.[22] The dye industry has long used ESIPT motifs imbued in dye formulations to extend the longevity of the coloration. As a control for ESIPT, the hydroxy groups were replaced with methoxy groups that reduce the stability of dimethylxylindein. Femtosecond transient absorption (fs-TA) of dimethylxylindein revealed a long-lived triplet excited state in DCM, explaining the instability due to reactive oxygen species.[23] To delineate the triplet state formation and decay dynamics, we performed fs-TA on dimethylxylindein in solution and thin films, aided by the ground/excited-

state femtosecond stimulated Raman spectroscopy (FSRS) to provide crucial structural information. This comprehensive study thus elucidates the excited-state potential energy surface of dimethylxylindein, formulating some relevant rational design principles to enhance SOC, ISC, and triplet formation for organic optoelectronic materials.

2. RESULTS AND DISCUSSION

2.1. Transient Electronic Signatures of Fungi-Derived Pigments in Solution. The excited-state electronic dynamics of dimethylxylindein and xylindein in solution up to ~4 ns show notable differences (Figure 1). The steady-state absorption peak of dimethylxylindein is blue-shifted from xylindein by ~100 nm, both displaying vibronic progression.[24,25] Dimethylxylindein has one broad fluorescence peak from the relaxed singlet excited state (S_1) resulting in a small Stokes shift, whereas xylindein emits at 709 and 846 nm assigned to protonated state (PA*) and ESIPT photoproduct, respectively (see Figure S1).[22] Moreover, the fluorescence quantum yields of dimethylxylindein (0.7%) and xylindein (<0.1%) are low in DCM.[23] Three prominent features in TA plots include blue excited-state absorption (ESA), ground-state bleaching (GSB), and red ESA bands. In xylindein (Figure 1b), all three bands decay similarly and disappear within ~100 picoseconds (ps). In contrast, some dimethylxylindein population remains excited as evidenced by an incomplete decay (recovery) of blue ESA (GSB), reminiscent of the TA spectra of thionated perylene diimides with a similar π-conjugated organic framework (an aromatic core) as a spectral signature for ultrafast triplet state formation,[24] although dimethylxylindein does not currently have any Group 16 elemental substitution. A close inspection reveals that the dimethylxylindein GSB is red-shifted by ~10 nm from the ground-state absorption (GSA, see Figure S2a for details) with altered vibronic peak spacing, whereas the xylindein GSB matches its GSA position.[22] Since this

peculiar red-shifted GSB is observed at long delay times (i.e., when red ESA mostly diminishes, see Figure 1a), it implies an intrinsic heterogeneity beneath the broad absorption profile of dimethylxylindein and a sub-population that is more prone to undergo ISC, likely with more nonplanar chromophore conformations to start with in the electronic ground state (see SI text following Figure S2 caption for an expanded discussion).

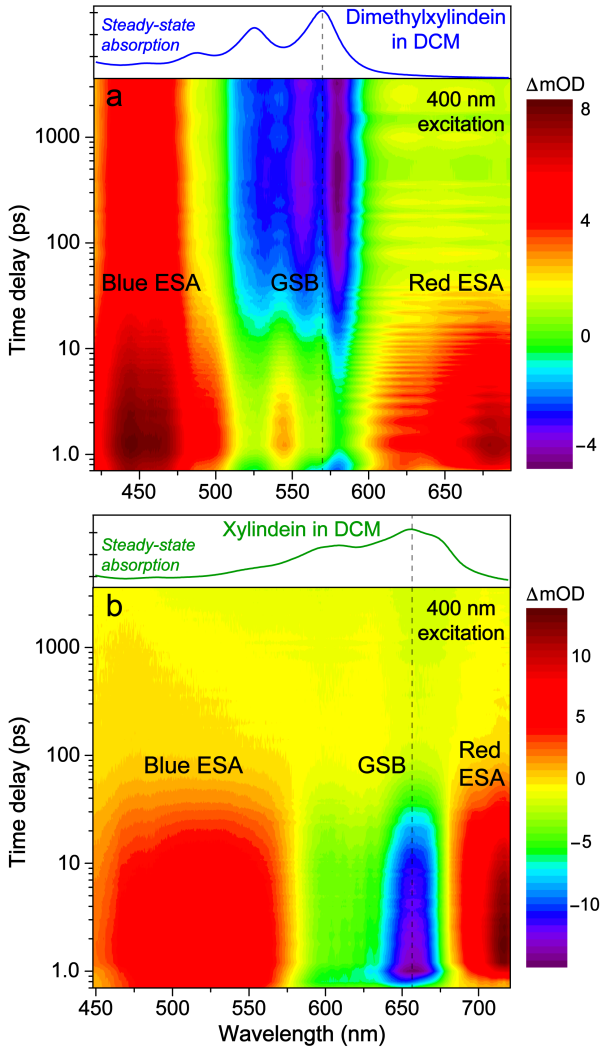

Figure 1. Semilogarithmic contour plots of fs-TA spectra after 400 nm excitation of (a) dimethylxylindein and (b) xylindein in DCM. The color-coded intensity levels are shown in milli-optical density (mOD) units to the right of each panel. Prominent transient electronic bands are labeled, and steady-state absorption spectra are displayed above each panel. The vertical dashed

lines highlight a red-shifted GSB peak from the ground-state absorption peak in (a) but not in (b) after the common 400 nm excitation.

Notably, the probe-dependent TA intensity dynamics of dimethylxylindein and xylindein show distinct patterns that are corroborated by global analysis (Figure 2).[26] The mirror-like dynamics of ESA bands (Figure 2d) and GSB (Figure 2f) infer a ~30 ps nonradiative decay of the singlet excited state (S_1) population to ground state (S_0) matching one dominant kinetic component (33 ps, Figure 2b), which was attributed to nonplanar motions of the molecular framework leading to a potential conical intersection.[22] In contrast, a parallel kinetic model was used for dimethylxylindein because of spectral overlap from multiple states, and three components were retrieved: ~1.6 ps, 18 ps, and 122 ns (Figure 2a) representing the initially excited CT state relaxation, conformational motions, and a triplet state lifetime, respectively (see Figure S2b for a sequential model). We note that the least-squares fitting to spectral data can retrieve characteristic time constants that go beyond the value corresponding to the delay stage length due to the nature of exponential decay functions (e.g., Figure 2c that yields different time constants on the ns timescale for blue and red ESA bands of the photoexcited chromophore). Red ESA band of dimethylxylindein primarily decays on the intermediate timescale (15 ps, Figure 2c), and given its molecular similarity to xylindein, the ~18 and 33 ps processes in these two chromophores may involve similar ultrafast distortions from the conjugated-ring planarity. The shortened time constant of dimethylxylindein relative to xylindein likely stems from the reduced intramolecular H-bonding from methyl substitution (Scheme 1), which makes the nonplanar motions more facile.[23]

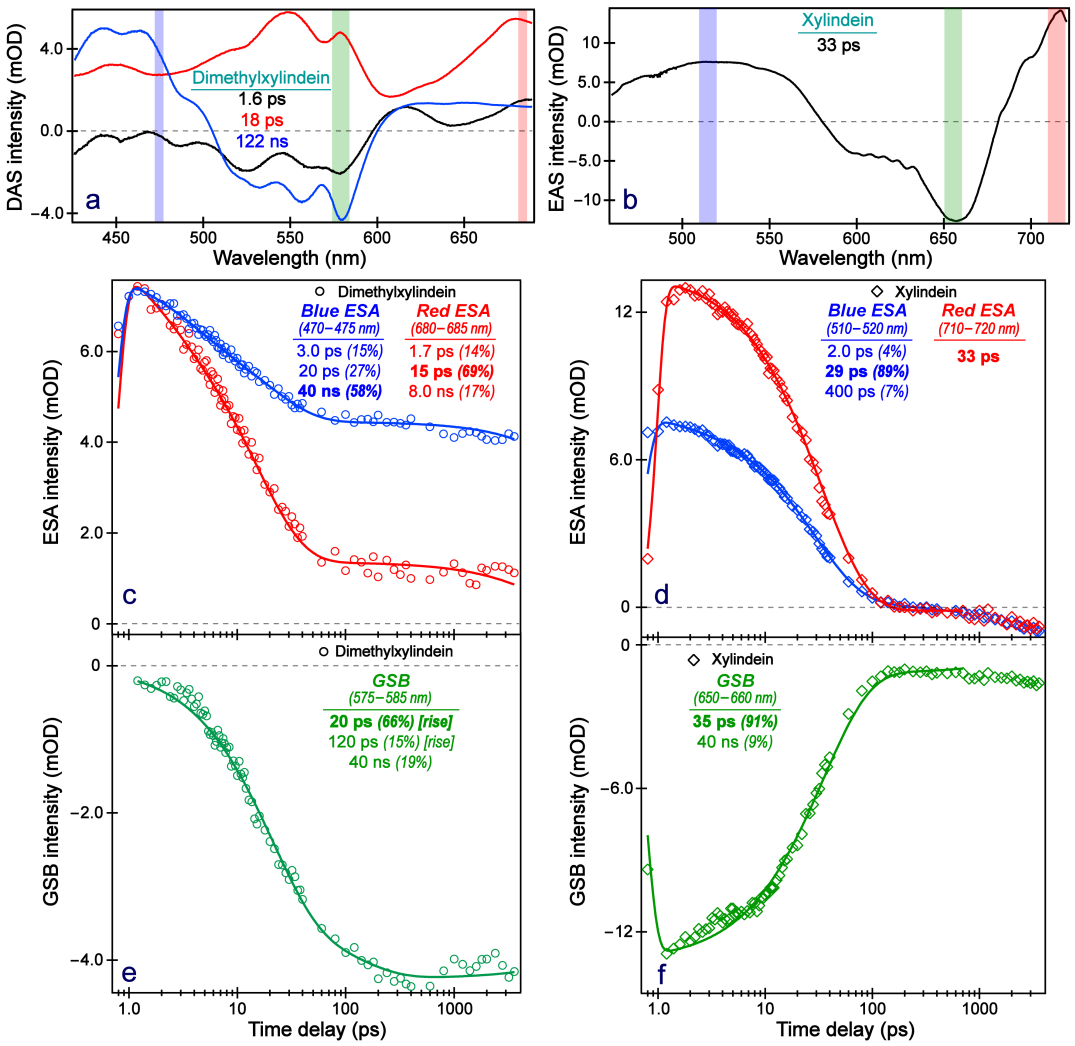

Figure 2. Global analysis and probe-dependent intensity dynamics of fs-TA spectra following 400 nm excitation. In the (a) decay-associated spectra (DAS) of dimethylxylindein (also see Figure S2b) and (b) evolution-associated spectra (EAS) of xylindein in DCM, the lifetimes are color-coded while shaded vertical bars highlight the signal integration regions for panels below. The ESA/GSB intensity dynamics of dimethylxylindein and xylindein are shown in (c)/(e) and (d)/(f), respectively. The least-squares fits (solid curves) are overlaid with data points, and color-coded time constants are listed with the dominant component bolded for each TA marker band.

However, the conformational motions of dimethylxylindein likely lead to a bifurcation of its excited-state population between a nonradiative $S_1 \rightarrow S_0$ transition (xylindein-like) and ISC to a triplet state (T_x). This bifurcation could explain the unusual and substantial GSB rise (66% weight, Figure 2e) with a 20 ps time constant, which is an "apparent rise" due to the spectrally overlapped concurrent ESA decay.[27] If the 20 ps process only involved a nonradiative downward transition, an effective cancellation of GSB/ESA decay would be observed with no apparent rise. Conversely, if this component solely represented ISC, a concurrent rise of a blue ESA band with more triplet-state character would be observed. Spectral overlap between $S_1 \rightarrow S_n$ and $T_1 \rightarrow T_n$ transitions renders mixed singlet/triplet states within blue ESA, which may mask its initial rise (blue trace, Figure 2c). Similarly, red ESA contains some singlet/triplet characters since the 8 ns long time constant (red trace, Figure 2c) was not observed in xylindein (red trace, Figure 2d). Such a direct comparison between xylindein and dimethylxylindein infers the effect of a single chemical substitution (–OH to $–OCH_3$). The small negative tails in blue and red ESA of xylindein are likely due to GSB and weak stimulated emission, respectively, which may obscure a longer fluorescent component.

2.2. Excitation Wavelength, Solvent Dependence, and Thin-Film Effect of Triplet Yield. To gain further insights into the excited-state dynamics of dimethylxylindein, we performed fs-TA experiments with 560 nm excitation to be more resonant with $S_0 \rightarrow S_1$ (Figure S3), instead of 400 nm excitation that populates S_n (see above). Besides an overall similar spectral pattern, an interesting difference lies in that blue ESA intensity is ~30% smaller than red ESA upon 560 nm excitation (Figure S4a), whereas both features have a largely equal intensity upon 400 nm excitation (Figure 2c). This unexpected result supports the importance of performing the excitation-dependent TA measurements and comparing the retrieved electronic dynamics that

report on photophysics and/or photochemistry pathways, which suggests that ultrafast ISC occurs more for dimethylxylindein in DCM with a bluer excitation, consistent with some literature that excitations to higher-lying electronic states could lead to higher triplet yields.[28,29] The reduction of the long-time components of blue, red ESA bands (25, 2.5 ns in Figure S4a) versus those of 400 nm excitation (40, 8.0 ns in Figure 2c) provides further evidence for diminishment of T_x formation after 560 nm excitation, although with a limited time window (see SI methods) this component likely represents an average S_1/T_1 lifetime with some uncertainty.

Though less soluble, dimethylxylindein was found to be stable in ethanol with little absorption loss over time, contrasting the significant absorption loss (photodegradation under white light in air) in DCM.[23] Since solute-solvent interactions can significantly impact energy dissipation, the fs-TA spectra of dimethylxylindein in ethanol after 400 nm excitation were collected (Figure S5). Surprisingly, the aforementioned long lifetime is replaced with a much shorter time constant (ca. 0.2–1.0 ns), typical of fluorescence pathway from S_1. The GSB profile matches GSA (Figure S2a) and nearly recovers within the time window, indicating that ISC is much reduced in ethanol. Such solvent dependence on triplet state formation is likely owing to polar solvents that raise the energy of T_{n+1} above S_n to greatly reduce ISC probability.[30,31] Moreover, the ~2.0 ps decay of the blue, red ESA shows a significantly increased magnitude in ethanol (48%, 39% in Figure S5c) compared to DCM (15%, 14% in Figure 2c) as the more polar ethanol can better stabilize a CT state.[31-33]

For applications of dimethylxylindein in optoelectronics, the thin film excited-state dynamics were examined (Figure S6). For thin-film xylindein, the ESA initial decay time constants (620 fs, 6.8 ps) are shorter than the dominant decay in solution (30 ps), indicating enhanced nonradiative decay upon excimer formation.[22,34-36] In contrast, thin-film dimethylxylindein dynamics (1.8 ps, 20 ps, 1.2 ns in Figure S6b) are similar to solution cases, especially in ethanol (1.3 ps, 25 ps, 2.1

ns in Figure S5b). The lack of excimer formation corroborates steady-state electronic properties as follows. First, with the solution concentration increase, dimethylxylindein does not aggregate like xylindein (see Figure S1 and the ensuing discussions).[22,23] Second, amorphous and crystalline dimethylxylindein thin films show about four orders of magnitude less conductivity (effective electron mobility) in the dark/ground state than amorphous xylindein thin films as we previously reported.[23] Third, dimethylxylindein shows about two orders of magnitude higher photosensitivity (charge photogeneration efficiency) than xylindein.[23] The decreased conductivity (with a reduced intra- and inter-molecular H-bonding network) and higher photosensitivity (no excimer formation) of thin-film dimethylxylindein than xylindein compliment the fs-TA data in this work (Figure S6).[22,23] Notably, the absence of a long lifetime in thin films infers quenching of ISC pathways. The time constants of dimethylxylindein in solution and thin films, although similar, exhibit distinct amplitude weights. The 1.5–2.0 ps decay of blue, red ESA has a higher weight in thin films (61%, 54%) than ethanol (48%, 39%) and DCM (15%, 14%), while the intermediate ~20 ps component is overall reduced (29%, 31%) relative to ethanol (29%, 42%) and DCM (27%, 69%). Therefore, transient CT state stabilization is likely enhanced when molecular conformational motions are more constrained (e.g., π-π stacking) in dimethylxylindein thin films, and the increased intra- and/or intermolecular CT character could be another factor responsible for the higher photosensitivity compared to xylindein.[22,23,35-37]

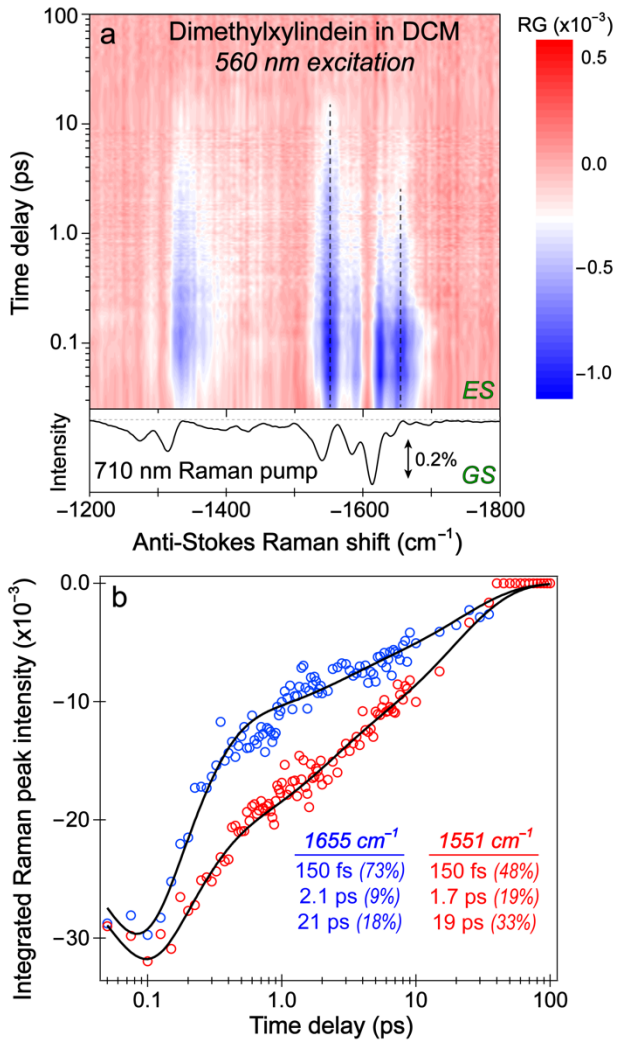

Figure 3. Transient vibrational features reveal non-equilibrium structural dynamics of the photoexcited chromophore. (a) Semilogarithmic contour plot of anti-Stokes excited-state (ES) FSRS of dimethylxylindein in DCM after 560 nm excitation (with 710 nm Raman pump). The ground-state (GS) FSRS is shown below. Color bar shows the stimulated Raman intensity in the excited state. The double-sided arrow denotes a Raman intensity of 0.2% in the ground state, the horizontal gray dotted line represents zero intensity. Vertical dashed lines track two prominent peaks with the integrated peak intensity dynamics at 1655 cm^{-1} (blue) and 1551 cm^{-1} (red) plotted in (b). Data points (circles) are overlaid with the least-squares fit (solid curve) on a logarithmic timescale. The retrieved time constants and amplitude weight percentages are listed.

2.3. Transient Vibrational Signatures of Dimethylxylindein in Solution. To provide structural characterization of the CT state, we implemented the anti-Stokes ground- and excited-state FSRS[25,38-40] on dimethylxylindein in DCM (Figures 3 and S7) which yielded pronounced vibrational signatures for the photosensitive molecular system in condensed phase.[41,42] The ground-state FSRS show prominent bands from 1550–1650 cm^{-1} mainly involving C=O and C=C stretching motions (see Table S1) as confirmed by calculations (Figure S9), and complemented by FSRS spectra comparing the GS/ES dimethylxylindein peaks (Figure S8a), GS dimethylxylindein in DCM/EtOH (Figure S8b), and GS dimethylxylindein/xylindein (Figure S8c). Besides a similar pattern, the ES peaks are blue-shifted from their GS counterparts (Figure S8a, Table S1), lending strong support to a CT state. Quantum calculations show that the lowest unoccupied molecular orbital (LUMO) accumulates electron density on the carbonyl groups and conjugated core compared to the highest occupied molecular orbital (HOMO). A majority of the blue-shifted peaks involve C=O and C=C stretch, supporting swift CT state formation upon photoexcitation.[25,43,44]

Two Raman bands above 1600 cm^{-1} decay faster than bands below 1600 cm^{-1}. With active roles during ES energy dissipation, strong peak intensities of ES marker bands (1655, 1551 cm^{-1}, Figure 3b) arise from large electric polarizability,[25] and their dynamics mostly match the red ESA decay (Figure 2c) on the 2–20 ps timescale. An initial ultrafast decay time constant (150 fs) is due to Franck-Condon relaxation:[25] the 1655 cm^{-1} peak decays more significantly than the 1551 cm^{-1} peak (73% versus 48% weight), while the former peak mainly involves C=O stretch and the latter peak mainly involves C=C stretch (Figure S10). Therefore, the peripheral carbonyl motions are likely more active during Franck-Condon relaxation and initial charge migration, while the C=C stretching motions participate primarily within the CT state as the core acquires more electron density, aided by analysis of other Raman peak dynamics (Figure S7). The chromophore core C=C

motions decay more on the ps timescale, which indicates that collective nonplanar core motions lead to a larger change of ES energetics than those induced by motions of the peripheral moieties.[22]

2.4. Excited-State Potential Energy Scheme for Dimethylxylindein in Solution. Based on the aforementioned results, a unifying energy level diagram is proposed (Figure 4). Upon 400 nm excitation, the populated S_n undergoes two relaxation pathways: ISC to T_n state or internal conversion to S_1', where the population may undergo further bifurcation akin to the 560 nm excitation case. Additional ISC pathways upon S_n excitation could explain why bluer excitation leads to more triplet formation via an ultrafast $S_n \rightarrow T_{n+1}$ transition (see SI text). The ISC from unrelaxed singlet states could occur within the cross-correlation time (~140 fs) of our laser setup[22,44] owing to the lack of peak wavelength shift and no additional rise of blue ESA characterizing the triplet state (Figure 1a). Ultrafast ISC has been observed in similar systems with appreciable $n\pi^*$ character, orbital mixing, and nonplanar structures or motions.[45-48]

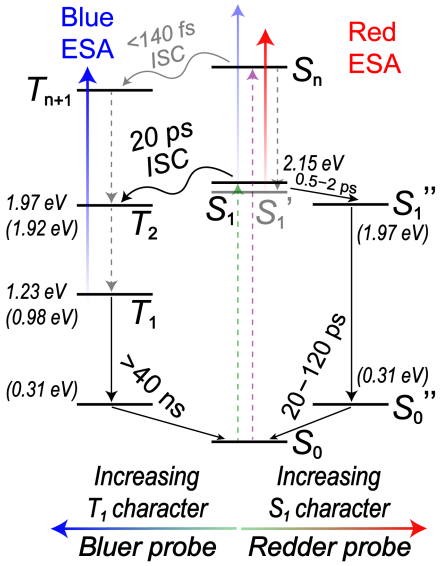

Figure 4. Energy level diagram for dimethylxylindein in DCM. Dashed purple and green vertical arrows represent 400 and 560 nm excitation, respectively. Intersystem crossing (ISC) from the

singlet (S_x) and triplet (T_x) states occurs over a range of timescales. S_1' and S_1'' represent relaxed S_1 states. The excited-state time constants listed are supported by time-resolved spectral data. Energy values in eV unit beside electronic states were calculated from unrelaxed excited states relative to the ground state (S_0), while energy values in parentheses were calculated from relaxed excited states relative to S_0. Vertical blue and red arrows represent blue and red excited-state absorption (ESA) bands, respectively. The probe wavelength gradient depicts the probe relative to ground-state absorption: a redder (bluer) probe observes the increasing S_1 (T_1) character.

Aside from ISC, the initially populated CT state (S_1') relaxes with an ~2 ps time constant,[33] which becomes shortened (500 fs, Figure S4a) when S_1 is directly populated by 560 nm excitation of dimethylxylindein in DCM. The relaxed ES population (S_1'') likely undergoes nonplanar structural motions (~20–120 ps, see Figures 2e and S4b) enabling a nonradiative return to GS, especially for dimethylxylindein in ethanol and thin films. Xylindein undergoes a similar process (~30 ps) following ESIPT,[22] so both pigments exploit this 20–30 ps process to effectively dissipate the photoexcitation energy and quench fluorescence.[23] However, the correlated ESA and GSB intensity dynamics of dimethylxylindein reveal that these conformational motions also promote ISC to triplet states, confirmed by the apparent rise of GSB with a conserved 20 ps time constant (Figure 2e). According to quantum calculations (see SI method), the energetic overlap between the relaxed S_1 ($^1\pi\pi^*$) and T_2 (more $^3n\pi^*$) states improves (with $\Delta E = 0.05$ eV in Figure 4) while the coordinate-dependent calculations show that these states become nearly isoenergetic as the chromophore structure becomes increasingly nonplanar and $n\pi^*$ character accumulates (Figure S11).[16,33] The increased orthogonality between the nonbonding electrons of C=O groups with the conjugated ring core could also improve SOC.[49,50] It is notable that although similar concepts

including slow/fast ISC pathways and nonplanar structural motions promoting ISC can be found in literature and various systems, rarely found is a comprehensive and concise display of these functional processes playing active roles in one molecular system (dimethylxylindein, see Figure 4), while being a naturally derived fungal pigment for sustainable optoelectronics.[22,23] Future investigations with a longer time window are necessary to accurately probe triplet lifetime (ca. 40–120 ns, Figure 2a,c,e) and attempt triplet quenching control experiments.[51] Additional solvent and temperature dependence studies on ISC may also provide illuminating insights.[52,53] Moreover, our fs-TA data on dimethylxylindein in DCM (Figure 1a) with interwoven control samples (e.g., in a different solvent EtOH, see Figure S5a; and thin films, see Figure S6a) in this work suggest that effective stabilization of a CT state could quench the ISC process, although ultrafast formation of a CT state may enhance ISC before the energy stabilization. That would be an interesting avenue of future research on related fungi-derived pigments in more solvents (if solubility allows) and various thin-film formats (e.g., with or without a polymer host matrix, different substrates).[23]

3. CONCLUSIONS

In summary, methylation of an organic optoelectronic material, xylindein, leads to ultrafast (<140 fs and ~20 ps) triplet state formation in DCM. The ISC of dimethylxylindein is enhanced relative to xylindein for multiple reasons; most importantly, xylindein in solution undergoes efficient ESIPT while thin films form excimers (through peripheral hydroxy groups), both of which quench the ISC pathway prevalent in dimethylxylindein. In particular, the methoxy groups of dimethylxylindein improve SOC and enhance ISC to the energetically close triplet state(s). With this being said, the avoidance of ESIPT is not the only and/or main reason we observe triplet state formation in dimethylxylindein, as the deprotonated xylindein with no dissociable proton still

decays with ~30 ps time constant and does not show detectable triplet state formation.[22] There are many systems which do not undergo ESIPT and still do not show appreciable ISC. For example, a methoxylated version of a popular photoacid pyranine called MPTS does not have a dissociable proton, which features a methoxy group and three sulfonate groups, yet it does not show any evidence for triplet state formation in solution.[54] These new results reinforce the need for foundational and fundamental research to perform experimental investigations and provide deep insights into the photophysics/photochemistry of complex functional organic molecules. Aside from the commonly known El-Sayed rule, further studies on the structural and electronic descriptors that affect the triplet formation dynamics are required. An interesting avenue to pursue is the fine balance between rigidity and flexibility of the certain-sized molecular structure in relation to the triplet formation. We reckon that a too flexible structure will lead to quenching of the ISC, while a too rigid structure will limit the distortions necessary to improve the SOC that promotes ISC. Moreover, the reduced H-bonding interactions to two symmetric methoxy groups likely promote conformational motions and nonplanarity, which supports better σ/π-orbital mixing for triplet formation. In the more polar ethanol, ISC is not energetically favored because the T_2 (T_{n+1}) states may be raised above the S_1 (S_n) states. Our fs-TA measurements of dimethylxylindein in ethanol and thin films confirm that stabilization of the CT state, which could lead to higher photosensitivity and charge photogeneration efficiency, and the constraint of out-of-plane distortions effectively quench ISC. Therefore, a balancing act needs to be optimized between CT state and triplet yield.

Looking forward, several rational design motives can thus be proposed to improve triplet yield in dimethylxylindein thin films by incorporating heterocyclic nitrogen or thionation to provide nonbonding lone pairs and enhance SOC.[14,24,47] The heavy-atom effect through halogen

substitution has also been used to enhance triplet formation,[55,56] though these electron-withdrawing substituents may facilitate CT formation and have other effects.[57] We note it is interesting that dimethylxylindein in DCM shows pronounced triplet state formation without heterocyclic nitrogen or thionation, and envision these substitutions at strategic atomic sites of the organic molecular framework could further boost the triplet yield in DCM and result in appreciable triplet states in thin films. The exploration of different photophysical scenarios with correlated electronic and structural dynamics insights[25] afforded by a strategic choice of solvents and thin films has enabled us to draw a comprehensive picture of the excited-state processes and establish important rules of molecular design for enhanced ISC. With such a mechanism-driven discovery feedback loop, the photosensitivity and optoelectronic performance can be efficiently improved to substantiate xylindein derivatives as low-cost, sustainable, and versatile optoelectronic materials.

ASSOCIATED CONTENT

Supporting Information. The Supporting Information is available free of charge on the ACS Publications website at http://pubs.acs.org.

Experimental methods including the materials and sample preparation, steady-state electronic and femtosecond transient absorption (fs-TA), tunable femtosecond stimulated Raman spectroscopy (FSRS), quantum calculations, Figures S1–S11 on the experimental and calculated electronic and vibrational properties of dimethylxylindein in solution and thin films after various excitations, Table S1 on mode assignment of key Raman bands of dimethylxylindein in DCM, additional references, and the full authorship of Gaussian 09 software (PDF)

AUTHOR INFORMATION

Corresponding Author

*E-mail: Chong.Fang@oregonstate.edu. Phone: 541-737-6704.

Notes

The authors declare no competing financial interests.

Author Contributions

Conceptualization, C.F. and O.O.; methodology (ultrafast spectroscopic toolsets and sample preparation), T.D.K., L.T., G.G., R.C.V.C., L.Z. and S.C.R.; software, T.D.K. and L.T.; formal analysis, T.D.K.; investigation, T.D.K., L.T., G.G., R.C.V.C. and L.Z.; visualization, T.D.K. and C.F.; writing—original draft, T.D.K. and C.F.; writing—review and editing, C.F. and O.O.; supervision, C.F.; funding acquisition, C.F., S.C.R. and O.O. All authors have read and agreed to the published version of the manuscript.

ACKNOWLEDGMENT

This work was supported by the U.S. National Science Foundation (NSF) grants CHE-2003550 and MCB-1817949 to C.F. We appreciate the NSF MRI development grant (DMR-1920368) for additional personnel support. This research was also funded by the NSF "Energy for Sustainability" program (CBET-1705099). T.D.K. acknowledges the Oregon Lottery Graduate Scholarship at Oregon State University (2020–2021). We thank Ryan Kim and Prof. Christopher Beaudry for the dimethylxylindein sample preparation, and Dr. Cheng Chen for helpful discussions.

REFERENCES

(1) Arias, A. C.; MacKenzie, J. D.; McCulloch, I.; Rivnay, J.; Salleo, A. Materials and Applications for Large Area Electronics: Solution-Based Approaches. *Chem. Rev.* **2010**, *110*, 3-24.

(2) Luo, J.; Huang, S.; Shi, Z.; Polishak, B. M.; Zhou, X.-H.; Jen, A. K. Y. Tailored Organic Electro-optic Materials and Their Hybrid Systems for Device Applications. *Chem. Mater.* **2011**, *23*, 544-553.

(3) Ostroverkhova, O. Organic Optoelectronic Materials: Mechanisms and Applications. *Chem. Rev.* **2016**, *116*, 13279-13412.

(4) Bronstein, H.; Nielsen, C. B.; Schroeder, B. C.; McCulloch, I. The Role of Chemical Design in the Performance of Organic Semiconductors. *Nat. Rev. Chem.* **2020**, *4*, 66-77.

(5) He, J.; Chen, H.; Hu, J.; Zhou, J.; Zhang, Y.; Kovach, A.; Sideris, C.; Harrison, M. C.; Zhao, Y.; Armani, A. M. Nonlinear Nanophotonic Devices in the Ultraviolet to Visible Wavelength Range. *Nanophotonics* **2020**, *9*, 3781-3804.

(6) Paolino, M.; Gueye, M.; Pieri, E.; Manathunga, M.; Fusi, S.; Cappelli, A.; Latterini, L.; Pannacci, D.; Filatov, M.; Léonard, J.; Olivucci, M. Design, Synthesis and Dynamics of a Green Fluorescent Protein Fluorophore Mimic with an Ultrafast Switching Function. *J. Am. Chem. Soc.* **2016**, *138*, 9807–9825.

(7) Li, M.; Li, Y.; Zhang, H.; Wang, S.; Ao, Y.; Cui, Z. Molecular Engineering of Organic Chromophores and Polymers for Enhanced Bulk Second-Order Optical Nonlinearity. *J. Mater. Chem. C* **2017**, *5*, 4111-4122.

(8) Köhler, A.; Bässler, H. Triplet States in Organic Semiconductors. *Mater. Sci. Eng. R Rep.* **2009**, *66*, 71-109.

(9) Shao, Y.; Yang, Y. Efficient Organic Heterojunction Photovoltaic Cells Based on Triplet Materials. *Adv. Mater.* **2005**, *17*, 2841-2844.

(10) Yost, S. R.; Hontz, E.; Yeganeh, S.; Van Voorhis, T. Triplet vs Singlet Energy Transfer in Organic Semiconductors: The Tortoise and the Hare. *J. Phys. Chem. C* **2012**, *116*, 17369-17377.

(11) Najafov, H.; Lee, B.; Zhou, Q.; Feldman, L. C.; Podzorov, V. Observation of Long-Range Exciton Diffusion in Highly Ordered Organic Semiconductors. *Nat. Mater.* **2010**, *9*, 938-943.

(12) Mikhnenko, O. V.; Blom, P. W. M.; Nguyen, T.-Q. Exciton Diffusion in Organic Semiconductors. *Energy Environ. Sci.* **2015**, *8*, 1867-1888.

(13) Van Court, R. C.; Giesbers, G.; Ostroverkhova, O.; Robinson, S. C. Optimizing Xylindein from *Chlorociboria* spp. for (Opto)electronic Applications. *Processes* **2020**, *8*, 1477.

(14) El-Sayed, M. A. Spin—Orbit Coupling and the Radiationless Processes in Nitrogen Heterocyclics. *J. Chem. Phys.* **1963**, *38*, 2834-2838.

(15) Baba, M. Intersystem Crossing in the $^{1}n\pi^{*}$ and $^{1}\pi\pi^{*}$ States. *J. Phys. Chem. A* **2011**, *115*, 9514-9519.

(16) Tang, L.; Fang, C. Nitration of Tyrosine Channels Photoenergy through a Conical Intersection in Water. *J. Phys. Chem. B* **2019**, *123*, 4915-4928.

(17) Saikawa, Y.; Watanabe, T.; Hashimoto, K.; Nakata, M. Absolute Configuration and Tautomeric Structure of Xylindein, A Blue–Green Pigment of *Chlorociboria* Species. *Phytochemistry* **2000**, *55*, 237-240.

(18) Robinson, S. C. The Fine Art of Decay. *Am. Sci.* **2014**, *102*, 206.

(19) Weber, G. L.; Boonloed, A.; Naas, K. M.; Koesdjojo, M. T.; Remcho, V. T.; Robinson, S. C. A Method to Stimulate Production of Extracellular Pigments from Wood-Degrading Fungi Using A Water Carrier. *Curr. Res. Environ. Appl. Mycol., J. Fungal Biol.* **2016**, *6*, 218-230.

(20) Harrison, R.; Quinn, A.; Weber, G.; Johnson, B.; Rath, J.; Remcho, V. T.; Robinson, S.; Ostroverkhova, O. Fungi-Derived Pigments as Sustainable Organic (Opto)electronic Materials. In *Proc. SPIE 10101, Organic Photonic Materials and Devices XIX, 101010U*, Proceedings of SPIE, May 5, 2017; Tabor, C. E., Kajzar, F., Kaino, T., Koike, Y., Eds.; SPIE: 2017.

(21) Giesbers, G.; Krueger, T.; Van Schenck, J.; Van Court, R.; Morré, J.; Fang, C.; Robinson, S.; Ostroverkhova, O. Fungi-Derived Xylindein: Effect of Purity on Optical and Electronic Properties. *MRS Adv.* **2019**, *4*, 1769-1777.

(22) Krueger, T. D.; Giesbers, G.; Van Court, R. C.; Zhu, L.; Kim, R.; Beaudry, C. M.; Robinson, S. C.; Ostroverkhova, O.; Fang, C. Ultrafast Dynamics and Photoresponse of a Fungi-Derived Pigment Xylindein from Solution to Thin Films. *Chem. Eur. J.* **2021**, *27*, 5627-5631.

(23) Giesbers, G.; Krueger, T. D.; Van Schenck, J. D. B.; Kim, R.; Van Court, R. C.; Robinson, S. C.; Beaudry, C. M.; Fang, C.; Ostroverkhova, O. Role of Hydroxyl Groups in the Photophysics, Photostability, and (Opto)electronic Properties of the Fungi-Derived Pigment Xylindein. *J. Phys. Chem. C* **2021**, *125*, 6534–6545.

(24) Tilley, A. J.; Pensack, R. D.; Lee, T. S.; Djukic, B.; Scholes, G. D.; Seferos, D. S. Ultrafast Triplet Formation in Thionated Perylene Diimides. *J. Phys. Chem. C* **2014**, *118*, 9996-10004.

(25) Fang, C.; Tang, L.; Chen, C. Unveiling Coupled Electronic and Vibrational Motions of Chromophores in Condensed Phases. *J. Chem. Phys.* **2019**, *151*, 200901.

(26) Snellenburg, J. J.; Laptenok, S. P.; Seger, R.; Mullen, K. M.; van Stokkum, I. H. M. Glotaran: A Java-Based Graphical User Interface for the R-Package TIMP. *J. Stat. Softw.* **2012**, *49*, 1-22.

(27) Gai, F.; Fehr, M. J.; Petrich, J. W. Observation of Excited-State Tautomerization in the Antiviral Agent Hypericin and Identification of Its Fluorescent Species. *J. Phys. Chem.* **1994**, *98*, 5784-5795.

(28) Stephansen, A. B.; Sølling, T. I. Distortion Dependent Intersystem Crossing: A Femtosecond Time-Resolved Photoelectron Spectroscopy Study of Benzene, Toluene, and *p*-Xylene. *Struct. Dyn.* **2017**, *4*, 044008.

(29) Isukapalli, S. V. K.; Lekshmi, R. S.; Samanta, P. K.; Vennapusa, S. R. Formation of Excited Triplet States in Naphthalene Diimide and Perylene Diimide Derivatives: A Detailed Theoretical Study. *J. Chem. Phys.* **2020**, *153*, 124301.

(30) Ley, C.; Morlet-Savary, F.; Jacques, P.; Fouassier, J. P. Solvent Dependence of the Intersystem Crossing Kinetics of Thioxanthone. *Chem. Phys.* **2000**, *255*, 335-346.

(31) Sonoda, Y.; Kwok, W. M.; Petrasek, Z.; Ostler, R.; Matousek, P.; Towrie, M.; Parker, A. W.; Phillips, D. Solvent Effects on the Photophysical and Photochemical Properties of (*E*,*E*,*E*)-1,6-bis(4-nitrophenyl)hexa-1,3,5-triene. *J. Chem. Soc., Perkin Trans. 2* **2001**, 308-314.

(32) Tang, L.; Zhu, L.; Wang, Y.; Fang, C. Uncovering the Hidden Excited State toward Fluorescence of an Intracellular pH Indicator. *J. Phys. Chem. Lett.* **2018**, *9*, 4969-4975.

(33) Lv, M.; Yu, Y.; Sandoval-Salinas, M. E.; Xu, J.; Lei, Z.; Casanova, D.; Yang, Y.; Chen, J. Engineering the Charge-Transfer State to Facilitate Spin–Orbit Charge Transfer Intersystem Crossing in Spirobis[anthracene]diones. *Angew. Chem. Int. Ed.* **2020**, *59*, 22179-22184.

(34) Naumann, W. Fluorescence Quenching by Excimer Formation: Quenching Constant Approximations for Excimer Formation-Dissociation by Classical Potential Models. *J. Chem. Phys.* **2005**, *123*, 064505.

(35) Brown, K. E.; Salamant, W. A.; Shoer, L. E.; Young, R. M.; Wasielewski, M. R. Direct Observation of Ultrafast Excimer Formation in Covalent Perylenediimide Dimers Using Near-Infrared Transient Absorption Spectroscopy. *J. Phys. Chem. Lett.* **2014**, *5*, 2588-2593.

(36) Son, M.; Park, K. H.; Shao, C.; Würthner, F.; Kim, D. Spectroscopic Demonstration of Exciton Dynamics and Excimer Formation in a Sterically Controlled Perylene Bisimide Dimer Aggregate. *J. Phys. Chem. Lett.* **2014**, *5*, 3601-3607.

(37) Pandey, L.; Risko, C.; Norton, J. E.; Brédas, J.-L. Donor–Acceptor Copolymers of Relevance for Organic Photovoltaics: A Theoretical Investigation of the Impact of Chemical Structure Modifications on the Electronic and Optical Properties. *Macromolecules* **2012**, *45*, 6405-6414.

(38) Liu, W.; Tang, L.; Oscar, B. G.; Wang, Y.; Chen, C.; Fang, C. Tracking Ultrafast Vibrational Cooling During Excited State Proton Transfer Reaction with Anti-Stokes and Stokes Femtosecond Stimulated Raman Spectroscopy. *J. Phys. Chem. Lett.* **2017**, *8*, 997–1003.

(39) Oscar, B. G.; Chen, C.; Liu, W.; Zhu, L.; Fang, C. Dynamic Raman Line Shapes on an Evolving Excited-State Landscape: Insights from Tunable Femtosecond Stimulated Raman Spectroscopy. *J. Phys. Chem. A* **2017**, *121*, 5428-5441.

(40) Chen, C.; Zhu, L.; Fang, C. Femtosecond Stimulated Raman Line Shapes: Dependence on Resonance Conditions of Pump and Probe Pulses. *Chin. J. Chem. Phys.* **2018**, *31*, 492-502.

(41) Dietze, D. R.; Mathies, R. A. Femtosecond Stimulated Raman Spectroscopy. *ChemPhysChem* **2016**, *17*, 1224–1251.

(42) Fang, C.; Tang, L.; Oscar, B. G.; Chen, C. Capturing Structural Snapshots during Photochemical Reactions with Ultrafast Raman Spectroscopy: From Materials Transformation to Biosensor Responses. *J. Phys. Chem. Lett.* **2018**, *9*, 3253–3263.

(43) Tominaga, K.; Walker, G. C.; Jarzeba, W.; Barbara, P. F. Ultrafast Charge Separation in ADMA: Experiment, Simulation, and Theoretical Issues. *J. Phys. Chem.* **1991**, *95*, 10475-10485.

(44) Taylor, M. A.; Zhu, L.; Rozanov, N. D.; Stout, K. T.; Chen, C.; Fang, C. Delayed Vibrational Modulation of the Solvated GFP Chromophore into a Conical Intersection. *Phys. Chem. Chem. Phys.* **2019**, *21*, 9728-9739.

(45) Aloïse, S.; Ruckebusch, C.; Blanchet, L.; Réhault, J.; Buntinx, G.; Huvenne, J.-P. The Benzophenone $S_1(n,\pi^*) \rightarrow T_1(n,\pi^*)$ States Intersystem Crossing Reinvestigated by Ultrafast Absorption Spectroscopy and Multivariate Curve Resolution. *J. Phys. Chem. A* **2008**, *112*, 224-231.

(46) Marazzi, M.; Mai, S.; Roca-Sanjuán, D.; Delcey, M. G.; Lindh, R.; González, L.; Monari, A. Benzophenone Ultrafast Triplet Population: Revisiting the Kinetic Model by Surface-Hopping Dynamics. *J. Phys. Chem. Lett.* **2016**, *7*, 622-626.

(47) Zobel, J. P.; Nogueira, J. J.; González, L. Mechanism of Ultrafast Intersystem Crossing in 2-Nitronaphthalene. *Chem. Eur. J.* **2018**, *24*, 5379-5387.

(48) Dobrowolski, J. C.; Karpińska, G. Substituent Effect in the First Excited Triplet State of Monosubstituted Benzenes. *ACS Omega* **2020**, *5*, 9477-9490.

(49) Okada, T.; Karaki, I.; Matsuzawa, E.; Mataga, N.; Sakata, Y.; Misumi, S. Ultrafast Intersystem Crossing in Some Intramolecular Heteroexcimers. *J. Phys. Chem.* **1981**, *85*, 3957-3960.

(50) Harriman, A.; Mallon, L. J.; Ulrich, G.; Ziessel, R. Rapid Intersystem Crossing in Closely-Spaced but Orthogonal Molecular Dyads. *ChemPhysChem* **2007**, *8*, 1207-1214.

(51) Mohr, M. A.; Kobitski, A. Y.; Sabater, L. R.; Nienhaus, K.; Obara, C. J.; Lippincott-Schwartz, J.; Nienhaus, G. U.; Pantazis, P. Rational Engineering of Photoconvertible Fluorescent

Proteins for Dual-Color Fluorescence Nanoscopy Enabled by a Triplet-State Mechanism of Primed Conversion. *Angew. Chem. Int. Ed.* **2017**, *56*, 11628-11633.

(52) Song, L.; Fayer, M. D. Temperature Dependent Intersystem Crossing and Triplet-Triplet Absorption of Rubrene in Solid Solution. *J. Lumin.* **1991**, *50*, 75-81.

(53) Reineke, S.; Baldo, M. A. Room Temperature Triplet State Spectroscopy of Organic Semiconductors. *Sci. Rep.* **2014**, *4*, 3797.

(54) Krueger, T. D.; Boulanger, S. A.; Zhu, L.; Tang, L.; Fang, C. Discovering a Rotational Barrier within a Charge-Transfer State of a Photoexcited Chromophore in Solution. *Struct. Dyn.* **2020**, *7*, 024901.

(55) Cui, G.; Fang, W.-h. State-Specific Heavy-Atom Effect on Intersystem Crossing Processes in 2-thiothymine: A Potential Photodynamic Therapy Photosensitizer. *J. Chem. Phys.* **2013**, *138*, 044315.

(56) Oberhofer, K. E.; Musheghyan, M.; Wegscheider, S.; Wörle, M.; Iglev, E. D.; Nikolova, R. D.; Kienberger, R.; Pekov, P. S.; Iglev, H. Individual Control of Singlet Lifetime and Triplet Yield in Halogen-Substituted Coumarin Derivatives. *RSC Adv.* **2020**, *10*, 27096-27102.

(57) Boulanger, S. A.; Chen, C.; Tang, L.; Zhu, L.; Baleeva, N. S.; Myasnyanko, I. N.; Baranov, M. S.; Fang, C. Shedding Light on Ultrafast Ring-Twisting Pathways of Halogenated GFP Chromophores from the Excited to Ground State. *Phys. Chem. Chem. Phys.* **2021**, *23*, 14636-14648.

TOC GRAPHIC

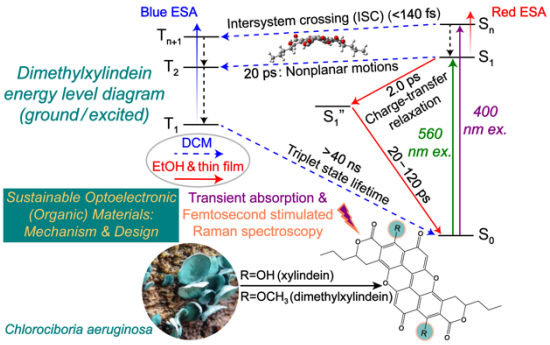
Blue ESA
Intersystem crossing (ISC) (<140 fs)
Red ESA
T_{n+1}
T_2
T_1
S_n
S_1
S_1"
20 ps: Nonplanar motions
2.0 ps
Charge-transfer
relaxation
400
nm ex.
560
nm ex.
20~120 ps
>40 ns
Triplet state lifetime
S_0
Dimethylxylindein
energy level diagram
(ground/excited)
DCM
EtOH & thin film
Sustainable Optoelectronic
(Organic) Materials:
Mechanism & Design
Transient absorption &
Femtosecond stimulated
Raman spectroscopy
R=OH (xylindein)
R=OCH$_3$ (dimethylxylindein)
Chlorociboria aeruginosa